PERGAMON

Solid-State Electronics 44 (2000) 1707–1710

SOLID-STATE ELECTRONICS

Technical Note

Analytic modeling of the subthreshold behavior in MOSFET

C.W. Liu *, T.X. Hsieh

Department of Electrical Engineering, National Taiwan University, 1, Section 4, Roosevelt Road, Taipei 10617, Taiwan, ROC

Received 30 November 1999; received in revised form 13 January 2000

Abstract

An analytic model is derived to describe the bias-dependent behavior of the subthreshold swing in MOSFETs for the uniform channel and the ion-implanted channel, and is compared to two-dimensional simulation, Tsividis' model and Brews' model. This simple analytical model confirms that the subthreshold swing is a function of the gate–source bias and exhibits a global minimum in the weak inversion region. This model is based on Tsividis' current equations and assumes that the surface potential difference between the drain and the source is small for the gate–source voltage below the threshold voltage. This yields a conventional exponential form of the subthreshold current, and the subthreshold swing can be obtained analytically from this current equation. © 2000 Elsevier Science Ltd. All rights reserved.

Keywords: Subthreshold current; Subthreshold swing

1. Introduction

The subthreshold swing is an important parameter to design high gain amplifiers [1], low voltage circuits [2], analog switches [3], and standby power dissipation in VLSI chips [4], where the MOSFETs are biased at weak inversion. The bias dependence of the subthreshold swing can cause nonlinear gain and distortion [5], degrading the circuit performance. Therefore, the accurate analytical modeling of the subthreshold swing is a prerequisite to design such circuits. Conventionally, the subthreshold current is assumed to be dominated by diffusion mechanism and an exponential dependence on gate–source bias is derived from a bipolar transistor argument [6]. However, the rigorous current equation for long channel MOSFETs has been given by Tsividis [7] in terms of the power of the surface potential at both drain and source. There seems to be a lack of linkage between these two forms of current equations. We, therefore, derived a mathematical pathway between these two models. The subthreshold swing St can be obtained by $\ln 10(\mathrm{d}\ln I_{\mathrm{DS}}/\mathrm{d}V_{\mathrm{GS}})$. A V_{GS}-independent St was given by [7,8]

$$\mathrm{St} = \phi_{\mathrm{t}} \ln 10\left(1 + \frac{\gamma}{2\sqrt{1.5\phi_{\mathrm{B}} + V_{\mathrm{SB}}}}\right), \quad (1)$$

where ϕ_{t} is thermal voltage, ϕ_{B}, the Fermi potential with respect to intrinsic Fermi level, and γ, the body factor. Brews also proposed a bias-dependent subthreshold swing [9]

$$\mathrm{St} = \phi_{\mathrm{t}} \ln 10\left(1 + \frac{C_{\mathrm{D}}(V_{\mathrm{GS}})}{C_{\mathrm{ox}}}\right), \quad (2)$$

where C_{ox} is gate-oxide capacitance and C_{D}, the depletion region capacitance, which is a function of gate–source bias in the subthreshold region. As a result, the Brews' subthreshold swing monotonically decreases with the gate–source bias. Recently, Vandamme et al. observed experimentally a global minimum of subthreshold swing [5], consistent with the two-dimensional simulation and the extraction from Tsividis' current equations [7]. However, an analytical expression of such subthreshold swing was not yet derived. We, therefore, derived the analytical form of such subthreshold swing, based on the previously derived subthreshold current.

* Corresponding author. Tel.: +886-2-2363521; fax: +886-2-2368247.

E-mail address: chee@cc.ee.ntu.edu.tw (C.W. Liu).

0038-1101/00/$ - see front matter © 2000 Elsevier Science Ltd. All rights reserved.

PII: S0038-1101(00)00116-7

2. Model description

With the assumption of long channel and uniformly doped NMOSFET, the positive surface potential (bending down toward Si/oxide interface) can be approximated by neglecting those exponential terms with negative surface potential [7]:

$$V_{\mathrm{GB}} = \psi_{\mathrm{X}} + V_{\mathrm{FB}} + \gamma\left(\psi_{\mathrm{X}} + \exp\left(\frac{-2\phi_{\mathrm{B}}}{\phi_{\mathrm{t}}}\right) \times \left[\phi_{\mathrm{t}}\exp\left(\frac{\psi_{\mathrm{X}} - V_{\mathrm{XB}}}{\phi_{\mathrm{t}}}\right) - \psi_{\mathrm{X}}\right]\right)^{1/2}, \tag{3}$$

where ψ_{X} is surface potential at the drain or source, V_{GB}, the gate–substrate voltage, and V_{FB}, the flat band voltage. In the subthreshold region, the difference between the drain and source potential is small and can be calculated approximately:

$$\begin{aligned}\varDelta &\equiv \psi_{\mathrm{D}} - \psi_{\mathrm{S}} \\ &= \gamma\sqrt{\psi_{\mathrm{S}}}\left(\sqrt{1 + \exp\left(\frac{-2\phi_{\mathrm{B}}}{\phi_{\mathrm{t}}}\right)\left[\frac{\phi_{\mathrm{t}}}{\psi_{\mathrm{S}}}\exp\left(\frac{\psi_{\mathrm{S}} - V_{\mathrm{SB}}}{\phi_{\mathrm{t}}}\right) - 1\right]}\right. \\ &\quad \left. - \sqrt{1 + \frac{\varDelta}{\psi_{\mathrm{S}}} + \exp\left(\frac{-2\phi_{\mathrm{B}}}{\phi_{\mathrm{t}}}\right)\left[\frac{\phi_{\mathrm{t}}}{\psi_{\mathrm{S}}}\exp\left(\frac{\psi_{\mathrm{D}} - V_{\mathrm{DB}}}{\phi_{\mathrm{t}}}\right) - 1 - \frac{\varDelta}{\psi_{\mathrm{S}}}\right]}\right) \\ &\approx \frac{\gamma\phi_{\mathrm{t}}}{2\sqrt{\psi_{\mathrm{S}}}}\exp\left(\frac{\psi_{\mathrm{S}} - 2\phi_{\mathrm{B}}}{\phi_{\mathrm{t}}}\right)\exp\left(-\frac{V_{\mathrm{SB}}}{\phi_{\mathrm{t}}}\right)\left(1 - \exp\left(-\frac{V_{\mathrm{DS}}}{\phi_{\mathrm{t}}}\right)\right)\left(1 + \frac{\gamma}{2\sqrt{\psi_{\mathrm{S}}}}\right)^{-1}.\end{aligned} \tag{4}$$

Eq. (4) is obtained by binomial expansion of the square root to the first order of $\varDelta$, and solving the linear equation of $\varDelta$. The difference is within 2% for the gate–source bias below the threshold voltage for a typical set of device parameters ($V_{\mathrm{DS}} = 3$ V, $t_{\mathrm{ox}} = 8.5$ nm, and substrate doping $N_{\mathrm{sub}} = 3 \times 10^{17}$ cm^{-3}), as shown in Fig. 1. Substituting Eq. (4) into Tsividis' current equations [7], we have

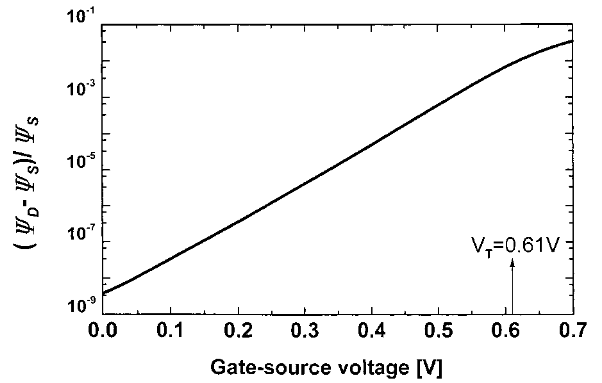

Fig. 1. Potential difference between drain and source as a function of gate–source voltage. $T = 300$ K, $t_{\mathrm{ox}} = 8.5$ nm, and $N_{\mathrm{sub}} = 3 \times 10^{17}$ cm^{-3}.

$$\begin{aligned}I_{\mathrm{drift}} &= \frac{W}{L}\mu C_{\mathrm{ox}}\left((V_{\mathrm{GB}} - V_{\mathrm{FB}})(\psi_{\mathrm{D}} - \psi_{\mathrm{S}}) - \frac{1}{2}(\psi_{\mathrm{D}}^2 - \psi_{\mathrm{S}}^2) - \frac{2\gamma}{3}\left(\psi_{\mathrm{D}}^{3/2} - \psi_{\mathrm{S}}^{3/2}\right)\right) \\ &\approx \frac{W}{L}\mu C_{\mathrm{ox}}\phi_{\mathrm{t}}\left(V_{\mathrm{GB}} - V_{\mathrm{FB}} - \psi_{\mathrm{S}} - \gamma\sqrt{\psi_{\mathrm{S}}}\right)\varDelta,\end{aligned} \tag{5}$$

$$\begin{aligned}I_{\mathrm{diff}} &= \frac{W}{L}\mu C_{\mathrm{ox}}\left(\phi_{\mathrm{t}}(\psi_{\mathrm{D}} - \psi_{\mathrm{S}}) + \gamma\phi_{\mathrm{t}}\left(\psi_{\mathrm{D}}^{1/2} - \psi_{\mathrm{S}}^{1/2}\right)\right) \\ &\approx \frac{W}{L}\mu C_{\mathrm{ox}}\phi_{\mathrm{t}}\varDelta\left[1 + \frac{\gamma}{2\sqrt{\psi_{\mathrm{S}}}}\right].\end{aligned} \tag{6}$$

The approximation in Eqs. (5) and (6) is done by the binomial expansions of power terms of ψ_{D} to the first order of $\varDelta$. The subthreshold current is the sum of drift and diffusion current, and can be transformed into the exponential form:

$$I_{\mathrm{DS}} = I_0(\psi_{\mathrm{S}})\exp\left(\frac{\psi_{\mathrm{S}} - 2\phi_{\mathrm{B}}}{\phi_{\mathrm{t}}}\right). \tag{7}$$

For the subthreshold swing calculation, the weak bias dependence of the prefactor, which is the lump sum and product of other nonexponential terms of ψ_{S}, is generally neglected. An analytical solution for subthreshold swing St can be obtained from the definition of $\mathrm{St} = \ln 10(\mathrm{d}\ln I_{\mathrm{DS}}/\mathrm{d}V_{\mathrm{GS}})$ as well as Eq. (3):

$$\mathrm{St} = \ln 10\phi_{\mathrm{t}} \times \left(1 + \gamma\frac{1 + \exp\left(\frac{-2\phi_{\mathrm{B}}}{\phi_{\mathrm{t}}}\right)\left(\exp\left(\frac{\psi_{\mathrm{S}}}{\phi_{\mathrm{t}}}\right) - 1\right)}{2\sqrt{\psi_{\mathrm{S}} + \exp\left(\frac{-2\phi_{\mathrm{B}}}{\phi_{\mathrm{t}}}\right)\left[\phi_{\mathrm{t}}\exp\left(\frac{\psi_{\mathrm{S}}}{\phi_{\mathrm{t}}}\right) - \psi_{\mathrm{S}}\right]}}\right). \tag{8}$$

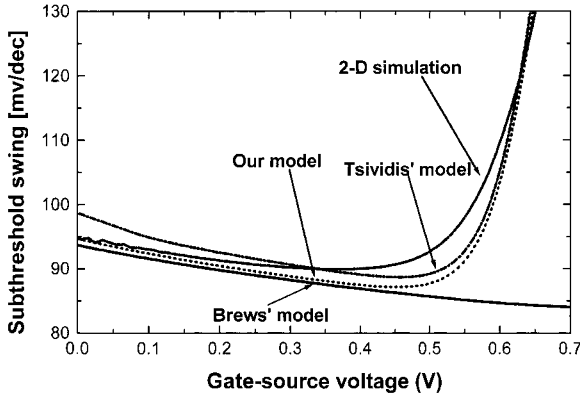

Fig. 2. Comparison of subthreshold swing extracted from Tsividis' model, Brews' model, our model and the two-dimensional simulation results: $T = 300$ K, $t_{ox} = 8.5$ nm, and $N_{sub} = 3 \times 10^{17}$ cm^{-3}.

3. Results and discussion

Fig. 2 shows the gate–source bias dependence of the subthreshold swing from our model for an NMOSFET, together with the Brews' model, the extracted subthreshold swing from Tsividis' current equations, and the subthreshold swing from the two-dimensional device simulation [10]. Our analytical model confirms the previously reported global minimum of the subthreshold swing on gate–source bias [5]. The difference between our analytical model and Tsividis' model is within 3 mV dec^{-1} in the subthreshold region. The surface potential ψ_{min} corresponding to the minimum subthreshold swing (St_{min}) can be obtained from the derivative of Eq. (8), and is a function of ϕ_B, independent of body effect parameter. In other words, it is determined by the substrate doping, independent of oxide thickness. The difference between $2\phi_B$ and ψ_{min} is plotted in Fig. 3 for reasonable ϕ_B region (0.3–0.5 V), and is relatively a constant (from 101 to 108 mV). The analytical value is slightly different from the previously reported value of 85 mV [5]. This relatively constant value of $2\phi_B - \psi_{min}$ yields the linear dependence between the V_{min} and V_T [5], which are the corresponding gate–source voltages for ψ_{min} and $2\phi_B$, respectively. Since a single and accurate value of subthreshold swing is required for most circuit modeling, we propose to use an inverse average of St to get such value:

$$I_{DS} = I_0 \exp\left(-\int_{V_{GS}}^{V_T} \frac{1}{\mathrm{St}} \mathrm{d}V_{GS} \right) = I_0 \exp\left(\frac{V_{GS} - V_T}{\mathrm{St}_{ave}} \right), \tag{9}$$

where I_0 is the drain current at threshold voltage. Using the same device parameters, we have $\mathrm{St}_{ave} = 1.087\mathrm{St}_{min}$, similar to Ref. [5], which is $1.1\mathrm{St}_{min}$.

To take the channel implantation into consideration [9,11], we assume that the channel doping is a uniform step profile with depth X_j with doping concentration N_I. We have

$$\frac{\mathrm{d}^2\psi}{\mathrm{d}x^2} = -\left(\frac{q}{\varepsilon_{Si}}\right)\left[-N_A(x) + p_{p0}\mathrm{e}^{-q\psi/kT} + N_D - n_{p0}\mathrm{e}^{q\psi/kT} \right],$$
$$N_A(x) = N_I(1 - u(x - X_j)) + N_A, \tag{10}$$

where $u(x)$ is the unit step function. The total charge can be obtained by integration with respect to potential:

$$Q_C = -\sqrt{2qN_A\varepsilon_0 k_{Si}} \left(\phi_t \mathrm{e}^{-\psi_S/\phi_t} + \psi_S - \phi_t + \mathrm{e}^{-2\phi_B/\phi_t}\left(\phi_t \mathrm{e}^{\psi_S/\phi_t} - \psi_S - \phi_t\right) + \frac{N_I}{N_A}\left(\frac{qX_j^2}{2\varepsilon_0 k_{Si}}(N_I - N_A) + \frac{qN_A}{\varepsilon_0 k_{Si}} w X_j \right) \right)^{1/2} \tag{11}$$
$$w = \sqrt{\frac{2\varepsilon_0 k_{Si}(\psi_S - \psi_{ii})}{qN_A}}, \quad \psi_{ii} = \frac{qN_I X_j^2}{2\varepsilon_0 k_{Si}},$$

where w is the new channel depth and ψ_{ii}, the potential contributed by implantation profile. Note that the last two terms in the square root is obtained from the depletion region approximation. The subthreshold swing can be solved, using Eq. (11) and $V_{GS} = V_{FB} + \psi_S + Q_C/C_{ox}$:

$$\mathrm{St} = \ln 10 \phi_t \left(1 + \gamma\sqrt{2qN_A k_{Si}\varepsilon_0} \frac{(1 + \exp(-2\phi_B/\phi_t)(\exp(\psi_S/\phi_t) - 1)) + \frac{X_j N_I}{w N_A}}{2|Q_C|} \right). \tag{12}$$

The St for the implanted channel is plotted in Fig. 4. The V_{min} increases with the implantation dose, since the threshold voltage increases with the implantation dose. Given the same implantation dose ($X_j N_I$), the minimum value of the subthreshold swing (St_{min}) is lower in the shallow implant ($X_j = 10^{-6}$ cm, $N_I = 4 \times 10^{17}$ cm^{-3} in Fig. 4) as compared to deep implant ($X_j = 4 \times 10^{-6}$ cm, $N_I = 10^{17}$ cm^{-3} in Fig. 4).

To apply this analytical model in the submicron devices, we can follow BSIMS3v3 [12] to add an extra term $(2\exp(-\mathrm{DVT1}\,L/\mathrm{lt}) + \exp(-\mathrm{DVT1}\,L/2\mathrm{lt}))\,(C_{dsc} + C_{dscd}V_{ds} + C_{dscb}V_{bseff})/C_{ox}$ to take the drain induced

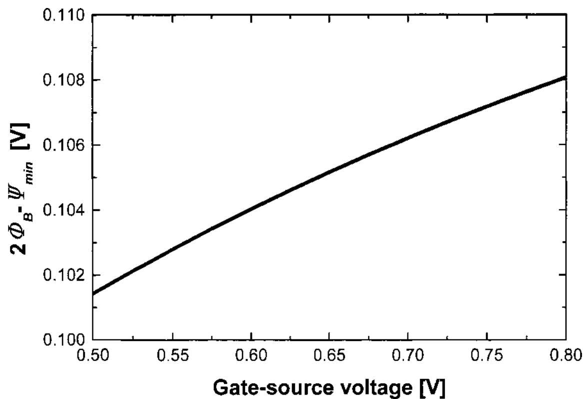

Fig. 3. The difference between the $2\Phi_B$ and surface potential, where subthreshold swing is minimum.

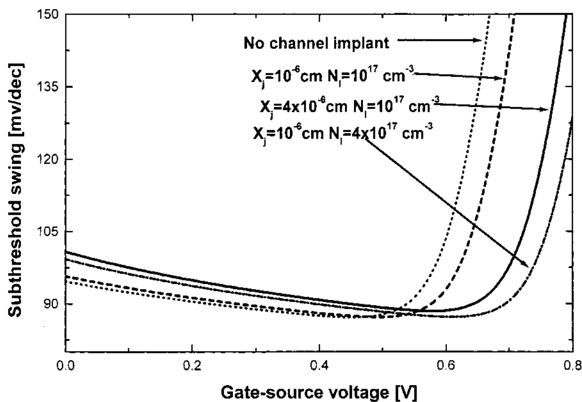

Fig. 4. The effects of channel implant under different implant conditions.

barrier lowering (DIBL) effect into account as long as the punch-through does not occur [13]. This term only slightly increases the subthreshold swing since the oxide capacitance is large for deep submicron devices. Another term C_{it}/C_{ox} can also be added to include the interface charge effect in the Si/SiO_2 interface.

4. Conclusion

The small difference between surface band bending at drain and source derives the exponential V_{GS} dependence of the subthreshold current and an analytical solution for subthreshold swing can be obtained. This analytical model predicts the subthreshold behaviors, similar to previously reported numerical and experimental results.

Acknowledgements

This work is supported by the National Science Council, Taiwan (NSC 88-2218-E-002-004)

References

[1] Laker K, Sansen W. Design of Analog Integrated Circuits and Systems. New York: McGraw-Hill; 1994.
[2] Mead C. Analog VLSI and Neural Systems. MA: Addison-Wesley; 1989.
[3] Aghtar S, Haslett JW, Trofimenkoff FN. Subthreshold analysis of an MOS analog switch. IEEE Trans Electron Dev 1997;44(1):89.
[4] Horiguchi M, Sakata T, Itoh K. Switched-source-impedance CMOS circuit for low standby subthreshold current giga-scale LSI's. IEEE J Solid-State Circuits 1993;28(11):1131.
[5] Vandamme EP, Jansen P, Deferm L. Modeling the subthreshold swing in MOSFET's. IEEE Electron Dev Lett 1997;18(8):369.
[6] Sze SM. Physics of Semiconductor Devices. 2nd ed. New York: Wiley; 1981.
[7] Tsividis T. Operation and modeling of the MOS transistor. New York: McGraw-Hill; 1988.
[8] Van Overstraeten RJ, Declerck GJ, Muls PA. Theory of MOS transistor in weak inversion-new method to determine the number of surface states. IEEE Trans Electron Dev 1975;22:282.
[9] Brews JR. Subthreshold behavior of uniformly and non-uniformly doped long-channel MOSFET. IEEE Trans Electron Dev 1979;26(9):1282.
[10] Silvaco Atlas, Two-Dimensional Simulation Program. ver.4.3.0.R.
[11] Swanson RM, Meindl JD. Ion-implanted complementary MOS transistors in low-voltage circuits. IEEE J Solid-State Circuits 1972;7(2):146.
[12] Cheng YH, Chan M, Chen K, Chen J, Huang JH, Liu ZH, Jeng MC, Hui K, Kuo PK, Hu C. BSIM3 version 3.0 manual. July 1995, University of California, Berkeley.
[13] Wolf S. Silicon Processing for the VLSI Era. Sunset Beach, CA. USA: Lattice Press, 1996. p. 242.